Ecological Applications, 20(2), 2010, pp. 508–524
© 2010 by the Ecological Society of America

Uncertainty propagation in an ecosystem nutrient budget

John C. Lehrter[1,4] and Just Cebrian[2,3]

[1]*U.S. EPA, NHEERL, Gulf Ecology Division, 1 Sabine Island Drive, Gulf Breeze, Florida 32561 USA*
[2]*Dauphin Island Sea Lab/University of Alabama, 101 Bienville Boulevard, Dauphin Island, Alabama 36528 USA*
[3]*Department of Marine Sciences, University of South Alabama, Mobile, Alabama USA 36688*

Abstract. New aspects and advancements in classical uncertainty propagation methods were used to develop a nutrient budget with associated uncertainty for a northern Gulf of Mexico coastal embayment. Uncertainty was calculated for budget terms by propagating the standard error and degrees of freedom. New aspects include the combined use of Monte Carlo simulations with classical error propagation methods, uncertainty analyses for GIS computations, and uncertainty propagation involving literature and subjective estimates of terms used in the budget calculations. The methods employed are broadly applicable to the mathematical operations employed in ecological studies involving step-by-step calculations, scaling procedures, and calculations of variables from direct measurements and/or literature estimates. Propagation of the standard error and the degrees of freedom allowed for calculation of the uncertainty intervals around every term in the budget. For scientists and environmental managers, the methods developed herein provide a relatively simple framework to propagate and assess the contributions of uncertainty in directly measured and literature estimated variables to calculated variables. Application of these methods to environmental data used in scientific reporting and environmental management will improve the interpretation of data and simplify the estimation of risk associated with decisions based on ecological studies.

Key words: *degrees of freedom; nutrient budget; salt marsh; standard error; uncertainty propagation.*

Introduction

The question of what constitutes the most reliable value to be assigned as the uncertainty of any given measured quantity is one that has been discussed for many decades and, presumably, will continue to be discussed. It is a question that involves many considerations and by its very nature has no unique answer. The subject of the propagation of errors, on the contrary, is a purely mathematical matter with very definite and easily ascertained conclusions. Although the general subject of the present article is by no means new, many scientists still fail to avail themselves of the enlightening conclusions that may often thus be reached, while others frequently use the theory incorrectly and thus arrive at quite misleading conclusions.

—Raymond T. Birge

This quote from the physicist Raymond T. Birge (1939) also opened a paper by Ku (1966) in which Ku lamented there was not a suitable reference in the literature or in textbooks on the subject of error propagation. Despite the general acknowledgement that quantitatively expressing uncertainty is important for the management of ecosystems (e.g., Regan et al. 2002, Halpern et al. 2006), very rarely is uncertainty rigorously treated in ecological studies (cf. Lo 2005, Cressie et al. 2009). Calls for uncertainty analysis in ecological risk assessment and decision making (e.g., Reckhow 1994) and for a greater emphasis on teaching of uncertainty analysis in ecological curricula (Brewer and Gross 2003) point to the need for uncertainty propagation methods that are accessible to ecologists. In this paper we reintroduce classical uncertainty propagation methods by demonstrating their use developing uncertainty intervals around all the terms in an ecosystem nutrient budget. These methods are relatively simple compared to many modern methods and are generally applicable to step-by-step calculations ubiquitous in the analysis of ecological data.

Manuscript received 4 December 2008; revised 6 May 2009; accepted 18 May 2009. Corresponding Editor: K. K. Treseder.
[4] E-mail: lehrter.john@epa.gov

Types of uncertainty and methods of uncertainty propagation

Uncertainty in the reporting of ecological results may be classified as either linguistic or epistemic (Regan et al. 2002). Linguistic uncertainty arises from miscommunication in the reporting and interpretation of data. Epistemic uncertainty is observational in nature and is described by measurement and systematic error, natural variability, inherent randomness, model uncertainty, and subjective judgment (i.e., best guesses). Uncertainties common to many problems include natural variability in observed variables, uncertainty about the model form that describes the problem, and uncertainty in model parameters (Chatfield 1995).

Of the epistemic uncertainties, measurement error and natural variability are the most rigorously quantified in ecological studies. Standardized methods for laboratory and field instruments serve to both minimize analytical error and enable the accurate reporting of uncertainty for analytical results. Statistical methods for quantifying natural variation in measurements of a population are routine. Methods for propagating model uncertainty, including both estimated model parameters and uncertainty in the functional form of a model, have been developed. Ultimately, hierarchical statistical models can incorporate and propagate all of the above types of uncertainty (e.g., Cressie et al. 2009).

The simplest calculations made with ecological data are step-by-step calculations, which do not involve model parameter estimation or model uncertainty. For example, the scaling of environmental measurements to a common length, area, or volume is ubiquitous in the ecological sciences. In fact, in the ecological sciences there are many routinely used functions that are based on first-principles and which have analytical solutions (i.e., no parameter estimation). Propagation of uncertainty associated with input variables to the output variables calculated with these functions may be accomplished using classical error propagation theory.

Classical error propagation theory

The classical error propagation equation (Birge 1939; elaborated by Tukey 1956, Ku 1966) propagates the error associated with input variables through a function. In the simplest case, $w = f(u, v)$, the propagated error of w is calculated as

$$s_w^2 = \left(\frac{\partial w}{\partial u}\right)^2 s_u^2 + \left(\frac{\partial w}{\partial v}\right)^2 s_v^2 + 2\frac{\partial w}{\partial u}\frac{\partial w}{\partial v}\mathrm{cov}(u, v) \qquad (1)$$

where s_w^2, s_u^2, and s_v^2 are the estimated variances of w, u, and v, respectively. The final term, cov(u, v), is the covariance where $\mathrm{cov}(u, v) = r_{uv}s_u s_v$, where r_{uv} is the correlation coefficient for the relationship between u and v. If the random errors in u and v are uncorrelated then the covariance term in Eq. 1 approaches zero and can be neglected (Ku 1966).

Eq. 1 is derived from the first-order Taylor series expansion of the normal distribution equation, and has been shown to be an accurate approximation when the following assumptions are satisfied: (1) input variables have approximately normal distributions and (2) the functional form of the equation does not possess derivatives of unreasonably large magnitude when evaluated at the averages for u and v (Ku 1966). When these assumptions cannot be satisfied, higher order terms from the Taylor series expansion may be required to obtain accurate estimates of s_w^2 (Tukey 1956). Use of Eq. 1 is dependent on knowing the analytical form of $f(u, v)$. In cases where $f(u, v)$ is not known, numerical methods may be necessary to propagate uncertainty (see *Methods: Measurements and budget calculations: Water surface elevation and embayment area, volume, and depth* and *Discussion: Modern uncertainty propagation methods*).

If the goal of error propagation is to develop confidence limits (CL) around a calculated variable, the standard error (SE) of the mean is the most appropriate error term to propagate as the SE may be converted directly to a CL by multiplying with a t value for a specified α and degrees of freedom (df). To differentiate between variables estimated as means from measured observations vs. variables calculated from two or more variables or estimated from the literature, we denote the mean of a directly measured variable U as $\overline{U}$. We denote the SE of the mean $\overline{U}$ as $\mathrm{SE}_{\overline{U}}$ which is calculated by the familiar

$$\mathrm{SE}_{\overline{U}} = \frac{s_U}{\sqrt{n}} \qquad (2)$$

where s_U is the standard deviation of the population U and n is the number of observations of U. The propagated SE of a parameter calculated as a function of two means, i.e., $W = f(\overline{U}, \overline{V})$ is denoted SE_W. Eq. 1 may be recast in terms of SE_W as

$$\mathrm{SE}_W = \left[\left(\frac{\partial W}{\partial \overline{U}}\mathrm{SE}_{\overline{U}}\right)^2 + \left(\frac{\partial W}{\partial \overline{V}}\mathrm{SE}_{\overline{V}}\right)^2 + 2r_{UV}\left(\frac{\partial W}{\partial \overline{U}}\mathrm{SE}_{\overline{U}}\right)\left(\frac{\partial W}{\partial \overline{V}}\mathrm{SE}_{\overline{V}}\right)\right]^{1/2}. \qquad (3)$$

In cases where U and V are uncorrelated, Eq. 3 may be simplified for sums, products, and quotients. For sums, $W = a\overline{U} \pm b\overline{V}$, Eq. 3 simplifies to

$$\mathrm{SE}_W = \sqrt{(a\mathrm{SE}_{\overline{U}})^2 + (b\mathrm{SE}_{\overline{V}})^2}. \qquad (4)$$

For products or quotients, $W = \overline{U} \times \overline{V}$ or $W = \overline{U}/\overline{V}$, Eq. 3 simplifies to

$$\mathrm{SE}_W = W\sqrt{\left(\frac{\mathrm{SE}_{\overline{U}}}{\overline{U}}\right)^2 + \left(\frac{\mathrm{SE}_{\overline{V}}}{\overline{V}}\right)^2}. \qquad (5)$$

Eqs. 4 and 5 may be used to propagate error for many simple step-by-step calculations in ecological analyses.

Uncertainty intervals and propagation of degrees of freedom

CLs for mean $\overline{U}$ are calculated by the familiar

$$\mathrm{CL} = \overline{U} \pm t_{(\mathrm{df},\alpha)}\mathrm{SE}_{\overline{U}} \qquad (6)$$

where t is the t statistic, obtained from a table of t values for the specified df and probability (α). The interval between the upper and lower confidence limits is the confidence interval (CI). If $\alpha = 0.05$, then 95% of the CIs constructed from samples of size n, repeatedly drawn from the population U, would contain the true mean.

The df may be thought of as the uncertainty around the uncertainty, such that for a large sample size there is less uncertainty about the SE and for a small sample size

the SE has greater uncertainty. Hence, for a small sample size the t value, for a specified α, is greater than the t value for a larger sample size. The df are calculated based on the number of estimated parameters. For example, $df = n - 1$ for a population mean and in the case of simple linear regression, where both a slope and intercept are estimated, $df = n - 2$.

A confidence interval for a parameter that is a function of other parameters may be calculated using the propagated SE and the propagated df. Recasting $W = f(\overline{U}, \overline{V})$ to the more general $W = f(\overline{W}_1, \overline{W}_2, \ldots, \overline{W}_j)$, the df for W (df_W) may be approximated using the Welch-Satterthwaite formula (Satterthwaite 1941, Welch 1947, Ku 1966). Similar to Eq. 3 we have replaced s^2 with SE to yield

$$df_W = \frac{SE_W^4}{\sum_{i=1}^{j} \frac{c_i^4 SE_{\overline{W}_i}^4}{df_{\overline{W}_i}}} \quad (7)$$

where $c \equiv \partial W/\partial \overline{W}_i$ and $df_{\overline{W}_i}$ are the degrees of freedom for $\overline{W}_i$. The assumptions for Eq. 7 are that variables are approximately normal, $SE_{\overline{W}_i}$ are statistically independent and

$$df_W \leq \sum_{i=1}^{j} df_{\overline{W}_i}. \quad (8)$$

Recent work indicates that the Welch-Satterthwaite approximation performs well for propagating df through calculations involving both directly measured and subjectively estimated variables (Hall and Willink 2001).

Strictly defined, the term "confidence interval" is applicable to variables or model parameters obtained from repeated sampling. Uncertainty propagated through a function of variables obtained by repeated sampling conforms to the interpretation of the CI (Taylor and Kuyatt 1994). Often, however, a variable or model parameter is subjectively estimated (i.e., obtained by means other than statistical analysis). Propagated uncertainty based on one or more subjectively estimated values does not conform to the strict interpretation of a CI, and in such cases the propagated uncertainty is often referred to as a "level of confidence" or "expanded uncertainty" (Taylor and Kuyatt 1994, International Organization for Standardization 1995). However, Hall and Willink (2001) demonstrate that the Welch-Satterthwaite formula performs very well when combining uncertainty from measured and subjectively estimated variables, and that the results may be interpreted as a confidence interval.

Application of uncertainty analysis to an ecosystem budget

Ecosystem mass budgets are an example of the class of ecological studies requiring step-by-step calculations and scaling. Nutrient budgets quantify nutrient sources and sinks and are a useful tool for cataloging nutrients dynamics in systems and evaluating the effects of management actions (Boynton et al. 2008). As it is not possible to measure all nutrient sources and sinks in an ecosystem, an ecosystem nutrient budget serves as a good example for illustrating how budget terms with propagated SE and df may be quantified from direct measurements, subjective literature estimates, and calculations. The field data presented in this work are a subset from a comparative study of three coastal embayments (cf. Stutes et al. 2007), and are used here to illustrate uncertainty propagation and the treatment of uncertainty.

This work builds upon a previous application of classical error propagation to ecological data (Lo 2005) by including propagation of the degrees of freedom. Further, we develop a novel method for the estimation of uncertainty in scaling variables such as area, volume, and depth calculated via GIS. We also demonstrate several examples of uncertainty estimation for literature estimates and subjective data.

In this treatment, we have ignored measurement, systematic, and model errors. Measurement errors are generally constrained by the use of appropriate instruments and well-trained operators. Systematic errors result from bias by instrument or sampling procedures and are usually small when instruments are well-calibrated and sample designs are appropriate for the research question. Model errors arise from the fact that models generally represent a simplified view of a system. For the relatively simple step-by-step and scaling calculations presented in this paper, natural variability in the observed and subjectively estimated variables is assumed to be the dominant error. Hence, the propagation of uncertainty associated with these variables is the focus of this paper.

Methods

Study site

An annual nutrient budget was constructed for the Gongora lagoon (30°18′18″ N, 87°25′26″ W) in northwestern Florida, USA (Fig. 1, Plate 1). The lagoon exchanges through a narrow mouth with the intercoastal waterway that connects Perdido Bay, Florida to Pensacola Bay, Florida. Salt marsh (primarily *Juncus roemerianus*) and maritime forest border the south side of the lagoon while houses and maritime forest border the north side. Anthropogenic modifications to the lagoon include a culvert that delivers storm water from a golf course at the northwestern end, bulkheads along the northern margin, and periodic dredging of a shallow central channel. Sampling stations in the lagoon were located along the central axis from the head of the embayment to its mouth in order to capture a salinity gradient. Sampling piezometers in the marsh and on the north side were located to capture horizontal gradients from uplands to the embayment. Shoalgrass (*Halodule wrightii*), which is abundant in nearby lagoons, is absent from the Gongora lagoon (Stutes et al. 2007).

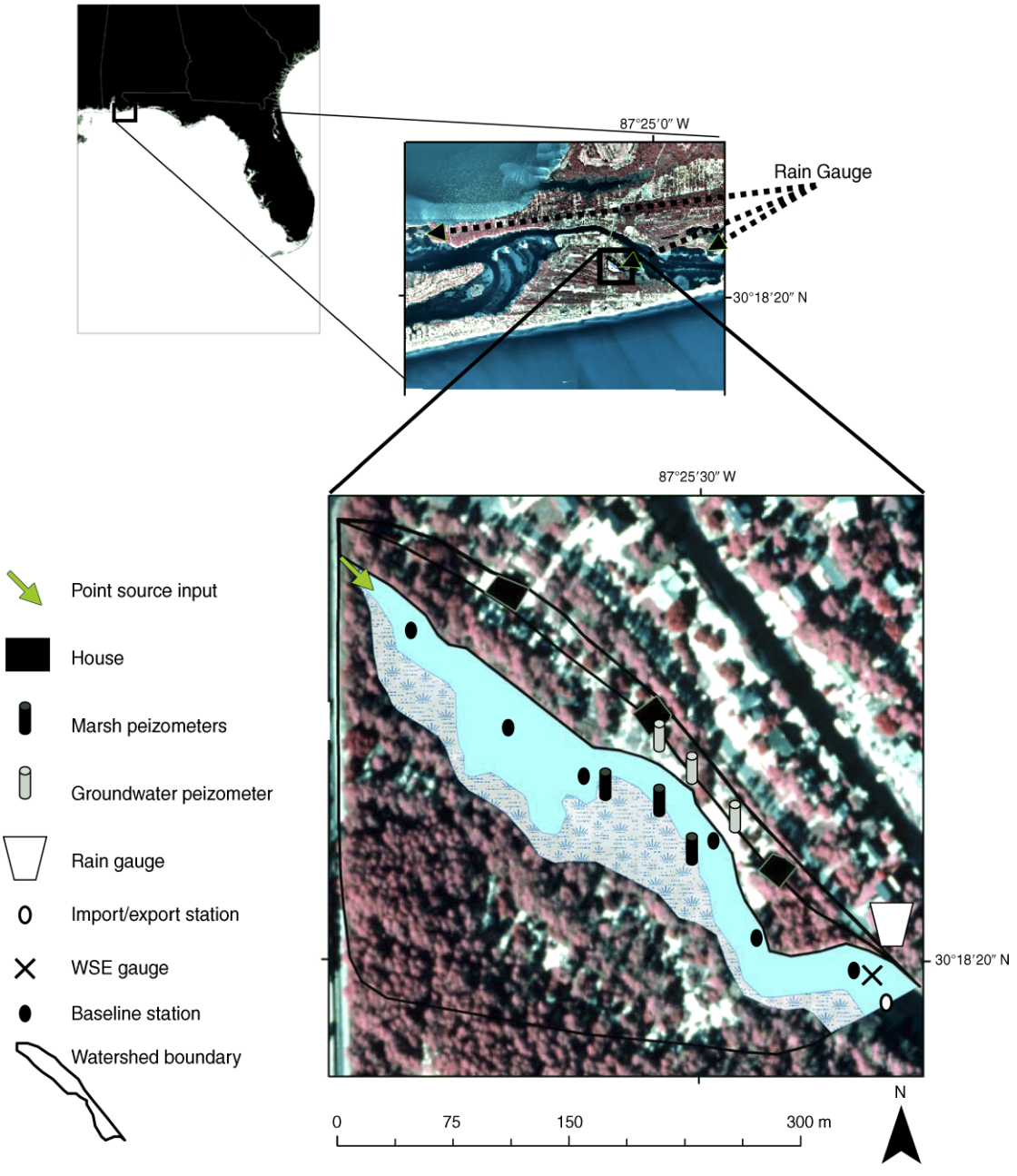

FIG. 1. Study location with sampling sites. WSE denotes water surface elevation.

Analytical methods

$NO_3^- + NO_2^-$, NO_2^-, NH_4^+, and PO_4^{3-} (dissolved inorganic phosphorus) were determined directly with colorimetric techniques (Strickland and Parsons 1972) modified for a Skalar SAN^{++} nutrient autoanalyzer (Skalar, Breda, The Netherlands). Total dissolved nitrogen (TDN) was determined by high temperature and chemical oxidation (D'Elia et al. 1977), and subsequent colorimetric measurement of $NO_3^- + NO_2^-$ on the Skalar SAN^{++} autoanalyzer. Dissolved inorganic nitrogen (DIN) was calculated as the sum of $NO_3^- + NO_2^-$ and NH_4^+. Dissolved organic nitrogen (DON) was calculated as the difference between TDN and DIN. Particulate nitrogen (PN) was measured after high temperature combustion (Sharp 1974) on a Carlo-Erba CNS analyzer (Carlo-Erba, Lakewood, New Jersey, USA).

Measurements and budget calculations

Field measurements were made over an annual cycle (1 July 2003 to 30 June 2004) at multiple locations in and around Gongora lagoon to characterize the seasonal and

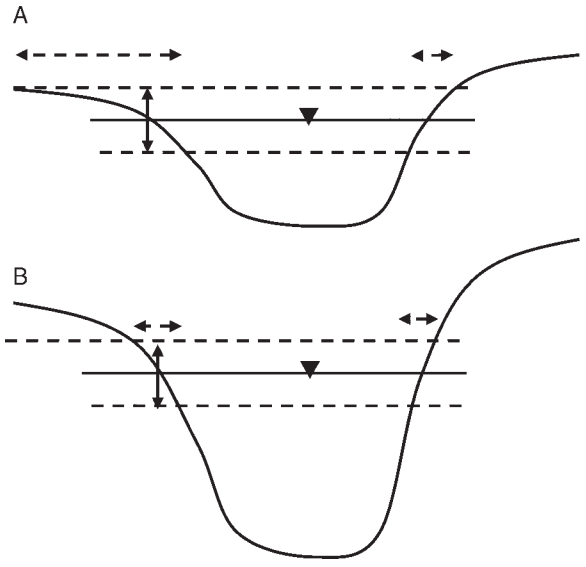

FIG. 2. Conceptual representation of how uncertainty in (A) water surface elevation (WSE) and (B) the triangulated irregular network (TIN) hull may affect estimates of surface area, depth, and volume. The triangles and the solid horizontal lines represent the estimated WSE. The dashed lines represent upper and lower limits of WSE, and the solid vertical arrows indicate the range of these limits. The horizontal dashed arrows indicate the potential differences in surface area based on the limits. In panel A, the uncertainty in area, volume, and depth is solely due to uncertainty in the WSE. Panel B has the same WSE as in panel A, but the shape of the embayment has been changed based on uncertainty in the TIN hull. This also affects the uncertainty in the area, volume, and depth.

spatial variability in the terms used to develop the annual nutrient budgets of DIN, DON, PN, and dissolved inorganic phosphorus (DIP). The nutrient budgets of DIN, DON, PN, and DIP were mass balanced as

$$\Delta S = \text{AtmDep} + \text{PS} + \text{GW} + \text{N-Ex} + \text{M-Ex} + \text{Black Box} \quad (9)$$

where ΔS was the change in storage, AtmDep was the atmospheric deposition, N-Ex was the net exchange (import − export) with the adjacent intercoastal waterway, PS was a point source input, GW was groundwater input, M-Ex was net exchange with the marsh adjacent to the embayment, and Black Box consisted of unmeasured sinks and sources. All sink and source terms were scaled to 1 m^2 of embayment and to an annual time scale.

Water surface elevation and embayment area, volume, and depth.—A pressure transducer (model WL16; Global Water, Inc., Gold River, California, USA) was installed at the mouth of the embayment (Fig. 1) to measure hourly water surface elevations (WSE). Hourly WSE were measured from April to December 2003. These hourly measured WSEs were used with concomitant hourly measurements at the nearby Pensacola Bay tide gauge (NOAA Station ID 8729840 referenced to vertical datum NAVD 88) to develop a linear regression model ($R^2 = 0.9$) for predicting WSEs for the period when WSEs at the study site were not measured.

Scaling of sinks and sources to the embayment area, volume, or depth was based on 3-D models of the embayment and surrounding watershed generated from point measurements and LIDAR-based elevation contours. Point elevations and horizontal position were measured with a real-time kinematic global positioning system (RTK GPS) instrument (Trimble 4800 GPS Total Station; Trimble, Sunnyvale, California, USA). The horizontal and vertical accuracy of the RTK GPS are on the order of 1 to 5 cm. Point elevation measurements were made in the embayment and surrounding areas with an aim to capture rapid changes in elevation associated with edges between the embayment and marsh, the embayment and bulkheads, and bathymetric gradients in the embayment associated with channels and shoals.

LIDAR elevation contour data (vertical accuracy = ±0.6 m) were obtained from Escambia County, Florida. The contours were converted to point values in a GIS (ArcGIS; ESRI, Redlands, California, USA) and adjusted to the same vertical datum as the RTK GPS data (NAVD 88). These two elevation layers were then combined to form a coverage of x, y, z point values spanning the embayment and its surrounding watershed. The resulting elevation coverage consisted of 8055 points. The elevation points were used to develop a 3-D surface of the study site using a universal kriging algorithm (ArcGIS Geostatistical Analyst extension).

To calculate areas and volumes, the 3-D digital surface was converted to a triangulated irregular network (TIN). The TIN hull was then used to calculate embayment areas and volumes at specified WSEs with the ArcGIS 3D Analyst extension. Areas (A) were calculated as a flat plane intersecting the specified WSE and being bounded in the x and y dimensions by the TIN hull (Fig. 2). The volume (V) beneath the flat plane was calculated by numerically integrating the TIN hull to the bottom vertical boundary. The embayment average depth (Z) was calculated as V/A.

The uncertainty of area and volume estimates was assessed by a novel multi-step method (Appendix A). The area and volume calculations were subject to uncertainty propagated from both the WSEs and the TIN hull generated through kriging (Fig. 2). As the algorithms for calculating the TIN hull with ArcGIS were not known, classical error propagation alone could not be used to determine errors in area and volume. Thus, error estimates for areas and volumes were calculated in a hybrid process that used both classical uncertainty propagation methods and a Monte Carlo approach (Appendix A).

ΔS.—Nutrient concentrations, salinity, and temperature were measured on seven sampling dates (approximately every two months) at six locations within the embayment (Fig. 1). Samples from each station were collected at mid-depth. Salinity and temperature mea-

TABLE 1. Methods for determining ecological variables with associated uncertainty. Listed along with each type of variable are the parameters of that type which were used to develop the nutrient budgets.

Method	Parameters used to develop nutrient budget
A) Direct measurements of a variable	
1) Location specific	x, y, z points, WSEs, $[C]_{last}$, $[C]_{first}$, $[R]$, Q_{PS}, [PS], [GW], $[I]$, $[E]$, T, S, [PW], [SW], Scarp
2) Region specific	P, Pensacola WSEs, P_{atm}
B) Direct calculation of a variable	
1) Calculation of a value from measured variables based on first principles	A_w, μ_0, μ_{SW}, D_0 and D_{SW} for NO_3^-, NO_2^-, and NH_4^+
2) Spatial or temporal scaling based on in site-specific regressions	A, V, Z, estimated WSEs, AMP, z, A_{flood}, F_{flood}
C) Subjective literature estimates of a variable	
1) Use many values from the literature	Dry : Wet, θ^2, pH
2) Use maximum and minimum values reported in the literature	ET, BD, %OM
3) Using a regression from the literature	PD, θ^2†
D) Calculation of a variable using literature estimates and first principles	D_0 and D_{SW} for DON and DIP

Note: Parameters are: x, y, z points, grid point values spanning the embayment and its surrounding watershed; WSEs, water surface elevations; $[C]_{last}$ and $[C]_{first}$, the average embayment concentrations of the nutrients dissolved inorganic nitrogen (DIN), dissolved organic nitrogen (DON), particulate nitrogen (PN), and dissolved inorganic phosphorus (DIP) from the last and first sampling dates, respectively; $[R]$, mean of rainfall nutrient concentrations among the three sites; Q_{PS}, discharge from the point source culvert; [PS] concentration of nutrient input from point source; [GW], measured groundwater nutrient; $[I]$, import nutrient concentration; $[E]$, export nutrient concentration; T, mean temperature of the embayment; S, salinity; [PW], porewater concentration of nutrients; [SW], surface water concentration of nutrients; Scarp, total scarp area; Pr, pressure; Pr_{atm}, mean atmospheric pressure; A_w, watershed area; μ_0, viscosity of freshwater; μ_{SW}, viscosity of sediment porewater; D_0, diffusion coefficient at infinite dilution in freshwater; D_{SW}, diffusion coefficient in soil porewater; A, embayment area; V, volume of the embayment; Z, average depth of the embayment; AMP, cumulative annual tidal amplitude; z, depth at which porewater was collected; A_{flood}, average area of marsh inundated per tidal cycle; F_{flood}, fraction of the year that the marsh was flooded; Dry : Wet, mean ratio of dry deposition to wet deposition; θ^2, squared tortuosity; ET, evapotranspiration; BD, bulk density of the marsh sediment; %OM, percentage of organic matter in soil; PD, particle density of marsh sediment.

† θ^2 was intended to be calculated by C3, but see *Methods: Measurements and budget calculations: M-Ex* for explanation of why it was calculated as a C1.

surements indicated the shallow water-column (mean depth was 0.48 m, see Appendix A) was well mixed.

Annual ΔS (mmoles·m^{-2}·yr^{-1}) for DIN, DON, DIP, and PN were calculated from embayment nutrient concentrations and embayment average depth as

$$\Delta S = \left(\frac{[\overline{C}]_{last} - [\overline{C}]_{first}}{\Delta t} \right) Z \qquad (10)$$

where $[\overline{C}]_{last}$ and $[\overline{C}]_{first}$ (mmoles/m^3) were the average embayment concentrations of DIN, DON, PN, and DIP from the last and first sampling dates, respectively, Δt was the time (yr) between the first and last sampling dates, and Z was the average depth (m) of the embayment. Uncertainty assessment for ΔS involved parameters that were directly measured or directly calculated (Table 1; Appendix B).

AtmDep.—Precipitation was measured with tipping-bucket rain gauges at three locations in the vicinity of the study embayment (Fig. 1). These locations provided an estimate of precipitation variability at the scale of the embayment. At these same locations, rainfall samples were collected in sterile jars during precipitation events. These samples were immediately frozen, and later analyzed for $NO_3^- + NO_2^-$, NO_2^-, NH_4^+, TDN, and DIP.

Annual AtmDep (mmoles·m^{-2}·yr^{-1}) for DIN, DON, and DIP were calculated as follows:

$$\text{AtmDep} = (\overline{P}[\overline{R}]) + (\overline{P}[\overline{R}]\text{Dry:Wet}) \qquad (11)$$

where $\overline{P}$ was the mean annual precipitation (m/yr) from the three precipitation gauges and $[\overline{R}]$ (mmoles/m^3) was the mean of rainfall nutrient concentrations (either DIN, DON, or DIP) among the three sites. Dry : Wet was the mean ratio of dry deposition to wet deposition.

The average Dry : Wet for DIN and DON (Table 1: C1) were calculated from wet and dry deposition data for other nearby estuaries; Mobile Bay, Mississippi Sound, and Apalachicola Bay (Meyers et al. 2001). The Dry : Wet for DIN ranged from 0.55 to 0.62 at these three sites, while for DON the Dry : Wet ranged from 0.20 to 0.27. The Dry : Wet for DIP is not as well constrained. Two previous studies in the State of Florida showed highly variable results with the mean Dry : Wet equaling 2.2 from an annual study in the Everglades (Ahn and James 2001) and 7.9 from a three-month study in Lake Okeechobee (Peters and Reese 1995). During a year-long study in Iowa, Anderson and Downing (2006) reported a mean Dry : Wet 4.2. For this study, the DIP Dry : Wet (Table 1: C1) was calculated as the mean of 2.2, 7.9, and 4.2. Uncertainty assessment for AtmDep involved parameters that were directly measured and

subjective estimates from the literature (Table 1; Appendix C).

PS.—A small culvert draining a storm water detention pond entered the embayment at its head (Fig. 1). The water exiting the culvert was sampled eight times over the study period for DIN, DON, PN, and DIP. The culvert had the shape of a rectangular box, which made it simple to calculate the discharge. The width of the culvert (0.48 m) and the depth of the water (1–15 cm) was measured along with the velocity (m/s) of the water flowing through the culvert on six occasions. The velocity was measured by simply timing how long it took a float to traverse a 1-m method of the culvert. The discharge (m^3/s) was then calculated as the product of the cross-sectional area of water (m^2) and the water velocity (m/s).

The annual PS inputs ($mmoles \cdot m^{-2} \cdot yr^{-1}$) of DIN, DON, PN, and DIP were calculated as

$$PS = \frac{\overline{Q_{PS}}\left[\overline{PS}\right]}{A} CF \quad (12)$$

where $\overline{Q_{PS}}$ (m^3/s) was the average measured discharge from the point source culvert, $\overline{PS}$ was the average concentration of DIN, DON, PN or DIP ($mmoles/m^3$), and A was the embayment area (m^2). CF was the conversion factor ($365 \times 86\,400$) for scaling the instantaneous flux to an annual scale. Uncertainty assessment for PS involved parameters derived as direct measurements or direct calculations (Table 1; Appendix D).

GW.—Groundwater samples were collected bimonthly from six piezometers installed in the upland area on the north side of the embayment (Fig. 1). The piezometers were arranged in pairs with one well being approximately 3 m from the water's edge and the next one being 8 m from the water's edge. The piezometers were constructed from PVC pipe (diameter = 2.54 cm), screened over a 10-cm interval, and installed to a depth of approximately 2 m below the surface. Plastic caps were placed on the bottom and top of the piezometer with the top cap being removed only for sampling. Prior to sample collection the piezometers were pumped dry three times with a hand pump.

Annual GW inputs ($mmoles \cdot m^{-2} \cdot yr^{-1}$) were determined as

$$GW = \frac{(\overline{P} - \overline{ET})A_w\left[\overline{GW}\right]}{A} \quad (13)$$

where $\overline{P}$ was the mean precipitation (m/yr), $\overline{ET}$ was the mean evapotranspiration (m/yr), A_w was the groundwater recharge area (m^2), $\overline{GW}$ was the mean of measured groundwater DIN, DON, PN, and DIP concentrations ($mmoles/m^3$), and A was the embayment area (m^2).

$\overline{ET}$ was estimated as the mean of minimum and maximum ET values reported for southeastern coastal plain watersheds (Lu et al. 2005). Minimum and maximum ET were found to be approximately 1.0 and 1.3 m/yr, respectively. The degrees of freedom approach infinity in cases where a parameter is the mean of estimated minimum and maximum values (see Taylor and Kuyatt 1994 for further discussion of this topic). In such cases we arbitrarily set df = 1000. This arbitrary decision was used as a way to hedge against the likelihood that estimated minimums and maximums were not the true extremes in the data. Even so, because large df have little impact on the propagated df and t values change minutely, for df > 1000 this decision has a very small impact on the propagated uncertainty interval.

A_w was assumed to equal the watershed area based on the assumption that the potentiometric slope of the surface of the unconfined groundwater aquifer mimicked the slope of the surface terrain (Dingman 1994). The elevation gradient of the watershed was complex due to the relic dune topography and, thus, it was difficult to accurately determine a watershed boundary. In order to accurately reflect the uncertainty in A_w, minimum and maximum watershed extents were determined using the LIDAR elevation data. The average A_w was calculated from the minimum and maximum extents with SE calculated from Eq. 2 and df set to 1000. The assessment of GW uncertainty involved direct measurements, direct calculations, and subjective literature estimates (Table 1; Appendix E).

N-Ex.—DIN, DON, PN, and DIP concentrations were measured at the mouth of the embayment (Fig. 1) during six rising tides (import) and six falling tides (export) throughout the study period. For each import or export event, four water samples were collected. Annual N-Ex ($mmoles \cdot m^{-2} \cdot yr^{-1}$) of DIN, DON, DIP, and PN between the lagoon and coastal waters was calculated from cumulative tidal exchanges and the measured nutrient concentrations as

$$N\text{-}Ex = \frac{1}{2} AMP([\tilde{I}] - [\overline{E}]) \quad (14)$$

where AMP was the cumulative annual tidal amplitude (m/yr) calculated from daily tidal amplitudes, and $[\tilde{I}]$ and $[\overline{E}]$ were the means of import and export concentrations ($mmoles/m^3$) for DIN, DON, PN, and DIP. This approach assumes that over an annual cycle the volume of the embayment is at steady state (i.e., incoming tidal volume = outgoing tidal volume). Under this assumption, the difference between $[\tilde{I}]$ and $[\overline{E}]$ drives N-Ex and AMP is simply a scaling term with associated uncertainty (Appendix F).

AMP was derived from hourly water surface elevation (WSE) measurements obtained at the mouth of the embayment from April to December 2003. These hourly measured WSEs were used in conjunction with hourly measurements at the nearby Pensacola Bay tide gauge (NOAA Station ID 8729840 referenced to vertical datum NAVD 88) to develop a linear regression model (see *Methods: Measurements and budget calculations: Water surface elevation and embayment area, volume, and depth*) predicting WSEs at Gongora for the January to June 2004 period. Daily maximum and minimum WSE

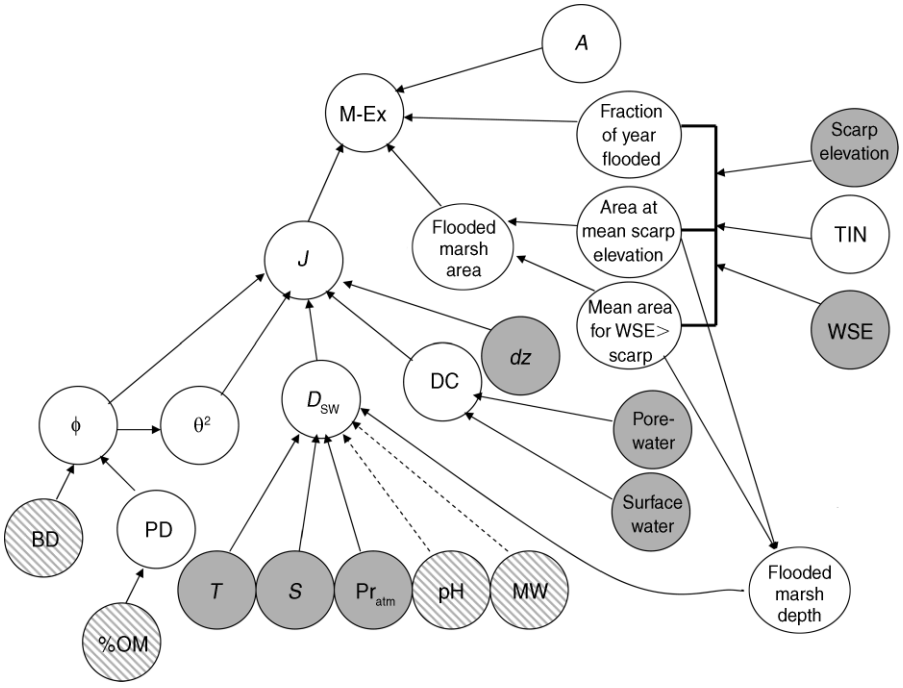

FIG. 3. Schematic representation of the step-by-step calculations used to determine the marsh exchange (M-Ex) term with associated uncertainty. Gray circles represent variables measured in this study, hatched circles represent variables estimated from the literature (subjective variables), and open circles are intermediate variables used in the final calculation of M-Ex with estimated uncertainty. Dashed arrows denote that pH was only used in the DIP calculation of D_{SW} and that MW was only used in the DON calculation of D_{SW}. See *Methods: Measurements and budget calculations: M-Ex* and Appendix G for definitions of the variables and the propagation of uncertainty.

values were extracted from the measured and predicted values and used to calculate a daily amplitude. Unfortunately the Pensacola WSE gauge did not acquire data from 4 April 2004 to 21 June 2004. Hence, AMP was calculated as

$$\text{AMP} = \frac{365}{N}\sum_{i=1}^{N}\text{daily amplitude}_i \qquad (15)$$

where N is the number of days (286) with either measured or regression-predicted values of WSE and $\Sigma_{i=1}^{N}$ daily amplitude$_i$ is the sum of the 286 daily amplitudes. The assessment of uncertainty in N-Ex involved direct measurements and direct calculations (Table 1; Appendix F).

M-Ex.—DIN, DON, and DIP porewater samples were collected bimonthly from six piezometers placed in the marsh adjacent to the embayment (Fig. 1). The piezometers were arranged in pairs with each pair consisting of one piezometer located in the marsh directly adjacent to the embayment (marsh edge) and one piezometer located 1 m away from the marsh edge. The marsh piezometers were constructed and sampled in a similar manner as the groundwater piezometers, the only difference being that the marsh piezometers were screened over a 5–15 cm depth interval below the marsh surface.

The derivation of M-Ex is most instructive of the theme of this work. The calculations involved make use of all the methods used here for determining ecological variables (Table 1). Further, the calculations serve as a good example of how uncertainty may be propagated through a complex model built upon step-by-step calculations that are ultimately scaled to a common dimension (Fig. 3). Annual M-Ex with the embayment (mmoles·m^{-2}·yr^{-1}) were calculated as

$$\text{M-Ex} = \frac{J \times A_{\text{flood}} \times F_{\text{flood}}}{A} \qquad (16)$$

where J (mmoles·m^{-2}·yr^{-1}) was the flux of DIN, DON, or DIP from the sediment porewater to the overlying surface water, A_{flood} was the average areal extent of marsh inundated per tidal cycle (m^2), F_{flood} was the fraction of the year that the marsh was flooded, and A was the embayment area (m^2). Uncertainty propagation equations are described in Appendix G.

J was calculated separately for NO_3^-, NO_2^-, NH_4^+, DON, and DIP by a diffusion model (Berner 1980, Boudreau 1997):

$$J = \phi\frac{D_{\text{SW}}}{\theta^2}\frac{dC}{dz} \times 3153.6 \qquad (17)$$

where ϕ was the porosity (dimensionless), D_{SW} was the porewater diffusion coefficient (cm^2/s), θ^2 was the

tortuosity squared (dimensionless), dC was the difference in concentration between the porewater and surface water (mmoles/m^3), and dz was distance between the depth of the surface sediment to the depth where the porewater was collected (m). As the piezometers were screened from 5 to 15 cm below the surface, dz was the average of these two depths (0.1 m). The number 3153.6 contains unit conversions. J for DIN was calculated as

$$J_{\mathrm{DIN}} = J_{\mathrm{NO_3^-}} + J_{\mathrm{NO_3^-}} + J_{\mathrm{NH_4^+}} \quad (18)$$

and ϕ was calculated by

$$\phi = 1 - \mathrm{BD}/\mathrm{PD} \quad (19)$$

where BD was the bulk density (g/cm^3) and PD the particle density (g/cm^3) of the marsh sediment. We obtained values of BD and PD using the SSURGO geospatial database (*available online*).[5] The marsh sediment in our study site was found to be Dirego muck soil which is described as highly organic coastal wetland soil. The BD was calculated as the mean of the maximum and minimum BD values for Dirego soils as determined from the SSURGO Escambia County, Florida database. The $\mathrm{SE_{BD}}$ was calculated using Eq. 2 and df was arbitrarily set to 1000. PD was calculated from a nonlinear empirical relationship that describes PD as a function of the percentage of organic matter content (Rühlmann et al. 2006; nonlinear model fitting was performed with S-PLUS statistical software). The percentage of organic matter (%OM) content for the Dirego soils at the Gongora site ranged from 25% to 60% (SSURGO). Using data provided by Rühlmann et al. (2006), we reproduced their nonlinear regression (Eq. 12 in Rühlmann et al. 2006) and used it to predict the PD at 25% and 60% OM. The mean PD was then calculated as the average of the PD predicted at 25% and 60% OM. The SE and df of the mean PD was propagated using Eqs. 3 and 7 based on the PD SE and df of the two predicted values obtained using the Rühlmann et al. (2006) data and regression.

We intended to estimate θ^2 as a function of ϕ using a regression model between these two variables (Boudreau 1996). To encompass the uncertainty associated with ϕ, the 99% upper and lower limit of ϕ were to be used as input to the model in a fashion similar to the derivation of PD. However, due to the large SE of ϕ (0.47), the upper and lower 99% limits fell outside the physical bounds on ϕ, which can only range from 0 to 1. Therefore, to encompass the uncertainty in ϕ we took the average of all the θ^2 values presented in Fig. 1 from Boudreau (1996), which showed θ^2 as a function of ϕ for systems similar to our study site. The θ^2 were obtained by digitizing the values in the figure, and the average, SE, and df were subsequently calculated.

D_{SW} was calculated from an approximate relationship (Li and Gregory 1974):

$$\frac{D_{\mathrm{SW}}}{D_0} \approx \frac{\mu_0}{\mu_{\mathrm{SW}}} \quad (20)$$

where D_0 was the diffusion coefficient at infinite dilution in freshwater, μ_0 was the viscosity of freshwater, and μ_{SW} was the viscosity of sediment porewater. Mean D_0 for each of NO_3^-, NO_2^-, NH_4^+, and DIP were calculated based on the mean temperature (T) of the embayment using the equations of Boudreau (1997). The speciation of DIP as either HPO_4^{2-} or $H_2PO_4^-$ was calculated based on porewater pH values measured in healthy coastal marshes in the Gulf of Mexico (McKee et al. 2006) and in the mid-Atlantic (Tyler and Zieman 1997, Kostka et al. 2002; J. Flory and M. Ogburn, *unpublished data*). The fractional contributions of the DIP species were used to calculate a weighted mean D_0 for DIP. Similar to a previous study (Alperin et al. 1992) the D_0 for DON was calculated based on diffusion coefficients and molecular weight data from different organic molecules presented by Jost (1960).

The parameters μ_0 and μ_{sw} were calculated using an approximation attributed to Matthaus (Boudreau 1997; Appendix G). This approximation calculates μ as a function of temperature (T), salinity (S, for $\mu_0 S = 0$), and pressure (Pr, millibars). Pr was calculated as

$$\mathrm{Pr} = \mathrm{Pr_{atm}} + (\rho \times g \times z) \quad (21)$$

where $\mathrm{Pr_{atm}}$ was the mean atmospheric pressure calculated from hourly readings from the Pensacola airport (about 30 km from the study site), ρ (kg/m^3) was the density of seawater, g was gravity, and z (m) was the mean depth of water overlying the marsh. Mean ρ was calculated as a function of mean T and S (Millero and Poisson 1981, UNESCO 1983; Appendix G).

The parameter dC was calculated as the difference between porewater concentrations and the surface water concentrations. Mean porewater concentrations ($\overline{[\mathrm{PW}]}$) were calculated from the piezometer samples and mean surface water concentration ($\overline{[\mathrm{SW}]}$) were calculated from water-column samples obtained in the embayment. The justification for using these measurements is that the diffusion gradients (dC) were driven by the concentrations in the embayment water that flooded the marsh.

The mean A_{flood} and the F_{flood} were determined from the RTK GPS measurements, the WSE data, and the TINs used to calculate embayment area. To differentiate between the marsh and the embayment, the mean elevation of the marsh–embayment interface or marsh scarp was determined from the RTK GPS measurements. During the RTK GPS survey, detailed measurements were made along rapid changes in elevation. Generally, there was an abrupt elevation change at the marsh edge (scarp), and thus, these regions were surveyed with particular care. Hourly WSEs that were statistically greater ($\alpha = 0.05$) than the mean scarp elevation were determined with Welch's approximate t test (Sokal and Rohlf 1995). Welch's t test is insensitive

[5] ⟨http://www.ncgc.nrcs.usda.gov/products/datasets/ssurgo/⟩

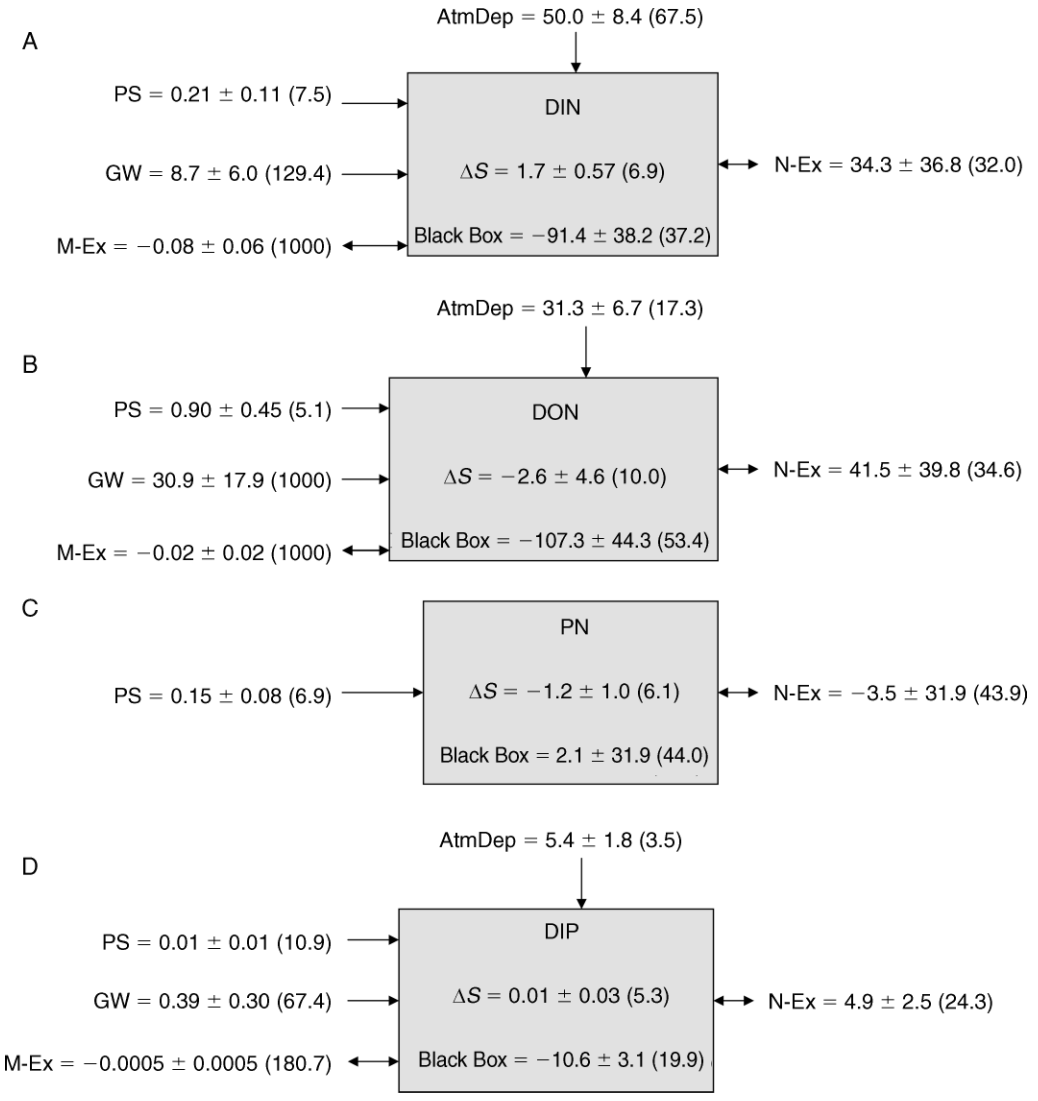

FIG. 4. Dissolved inorganic nitrogen (DIN), dissolved organic nitrogen (DON), particulate nitrogen (PN), and dissolved inorganic phosphorus (DIP) nutrient mass balance terms with propagated uncertainty (±SE; with df in parentheses). All units are mmol·m^{-2}·yr^{-1}. Positive terms represent an input to the embayment, while negative terms represent an output. Variables are: AtmDep, atmospheric deposition; PS, point source input; GW, groundwater input; M-Ex, net exchange with the marsh adjacent to the embayment; ΔS, the change in storage; Black Box, unmeasured sinks and sources; and N-Ex, net exchange (import − export) with the adjacent intercoastal waterway.

to different df as was the case with WSE and scarp elevation.

The WSEs that exceeded the scarp elevation were used in two ways. First, the number of hours when the marsh was flooded was used to calculate F_{flood}. Second, the WSEs exceeding the scarp height were used to calculate the area and volume of water flooding the marsh in a manner similar to the calculation of embayment area and volume (see *Methods: Measurements and budget calculations: Water surface elevation and embayment area, volume, and depth* and Appendix G). The mean A_{flood} was calculated as follows:

$$A_{\text{flood}} = (\text{mean area for WSE greater than mean scarp elevation}) - (\text{mean area at mean scarp elevation}). \quad (22)$$

The parameter V_{flood}, the volume of flooded marsh, was calculated similar to A_{flood} and the depth of the flooded marsh (Z_{flood}) was $V_{\text{flood}}/A_{\text{flood}}$.

Black Box terms.—To close the nutrient budgets, a Black Box term was calculated for DIN, DON, PN, and DIP from Eq. 9. This term includes all unmeasured processes ± uncertainty (Appendix H).

Results

DIN

AtmDep (50.0 mmoles·m^{-2}·yr^{-1}) and N-Ex (34.3 mmoles·m^{-2}·yr^{-1}) were the largest input terms in the DIN budget (Fig. 4A). However, the uncertainty around the N-Ex was so large (SE = 36.8) that the term was not significantly different from zero. GW inputs were relatively large in magnitude (8.7 mmoles·m^{-2}·yr^{-1}), but also had large uncertainty (SE = 6.0). PS, M-Ex, and ΔS were small budget terms with large uncertainties relative to the magnitude of the terms. The Black Box term was the largest output term (–91.4 mmoles·m^{-2}·yr^{-1}).

DON

Similar to the DIN budget, AtmDep (31.3 mmoles·m^{-2}·yr^{-1}) and N-Ex (41.5 mmoles·m^{-2}·yr^{-1}) were the largest input terms in the DON budget (Fig. 4B). GW input (30.9 mmoles·m^{-2}·yr^{-1}) was comparable to AtmDep and N-Ex, with GW and N-Ex both having large uncertainty. DON AtmDep and N-Ex inputs were of similar magnitude as DIN AtmDep and N-Ex inputs. DON GW input was approximately three times larger than DIN GW input, although these two inputs were not significantly different at $\alpha = 0.05$ owing to the large uncertainties around these terms. PS, M-Ex, and ΔS were small and had large uncertainties relative to their magnitude The Black Box term was the largest DON output term (–107.3 mmoles·m^{-2}·yr^{-1}).

PN

Contrary to the budgets for dissolved nitrogen, N-Ex (–3.5 mmoles·m^{-2}·yr^{-1}) was the largest output and the Black Box term (2.1 mmoles·m^{-2}·yr^{-1}) was the largest input in the PN budget (Fig. 4C). For all of the PN terms, however, the uncertainties were large relative to the magnitude of the terms, which resulted in none of the terms being significantly different from zero at $\alpha = 0.05$. PN N-Ex and Black Box terms were very small in comparison to DIN and DON N-Ex and Black Box terms.

DIP

DIP terms (Fig. 4D) showed similar trends as with DIN and DON. AtmDep (5.4 mmoles·m^{-2}·yr^{-1}) and N-Ex (4.9 mmoles·m^{-2}·yr^{-1}) were the dominant input terms, and the Black Box (–10.6 mmoles·m^{-2}·yr^{-1}) was the dominant output term. Due to large uncertainties, however, neither AtmDep nor N-Ex were significantly different from zero.

Discussion

The assumptions of the classical equations for propagating uncertainty

There are assumptions in the error (Tukey 1956, Ku 1966) and df (Welch 1947) propagation equations (Eqs. 1 and 7) that impact the accuracy of the propagated uncertainty. These assumptions include (1) input variables with approximately normal distributions and (2) well-behaved functions with derivatives that are not unreasonably large.

As regards the first assumption, for large sample sizes one can generally assume the normality of mean values based on the Central Limit Theorem. Even for small sample sizes, means of samples drawn from normally distributed populations are also normal. Ecosystem field measurements frequently suffer from small sample sizes, as is the case for many of the variables in this study, and usually there is not a priori knowledge of distributions. Many biological and physical phenomena, however, result in data distributions that are approximately normal. Further, as discussed by Ku (1966), Eq. 1 is "exact" only when the input variables come from exactly normal distributions. Thus, it is important to recognize that uncertainty estimates based on means from small sample sizes are themselves approximations.

For assumption 2, the simple functions used in this study preclude any of the derivatives being excessively large. For simple functions such as sums the higher order terms disappear and for products, quotients, roots, and small powers the accuracy of Eq. 1 is generally adequate as the higher order terms are much smaller than the error calculated by Eq. 1 (Ku 1966). For other functional forms, the higher order terms of the Taylor series should be evaluated (Tukey 1956). In mathematical terms, Eqs. 1 and 7 are accurate when assumptions 1 and 2 are met. In practical terms, previous work provides evidence that the error and df propagation equations are fairly robust even when the above assumptions are poorly met (Tukey 1956, Ku 1966).

Modern uncertainty propagation methods

As described by Chatfield (1995), there are three primary types of uncertainty encountered in the analysis of any problem: natural variation in observed variables, uncertainty about the form of the model that adequately describes the problem, and uncertainty in the model parameters.

Classical methods for propagating uncertainty have their origins in the physical sciences and engineering. In these disciplines, there is usually little uncertainty around model formulations. This is also true of simple calculations that are frequently conducted during the analysis of environmental data. For example, the calculation of rainfall nitrogen deposition is simply the product of precipitation and rainfall nitrogen concentration (first term on the right side of Eq. 11). There is little uncertainty around the form of this function and there are no model parameters to be estimated. For simple step-by-step calculations and scaling procedures the classical equations provide a straightforward method for propagating uncertainty, and, in contrast to more modern uncertainty propagation methods, are relatively simple.

Uncertainties around model form and model parameters may be addressed by modern frequentist and Bayesian methods. The difference between a Bayesian and a frequentist analysis is that the Bayesian approach employs the mathematics of probability distributions for a model parameter and specifies a prior probability for a parameter based on a "degree of belief" (de Valpine 2009). In a Bayesian approach, parameters with uncertainty are incorporated into a model by integrating over all the possible parameter values. The calculation of these integrals to develop a posterior distribution usually requires computationally intensive numerical integration methods such as Markov chain Monte Carlo (MCMC). MCMC algorithms for Bayesian analyses are often implemented from software, such as WinBUGS, specifically designed for this purpose (Gilks et al. 1994).

In contrast to Bayesian methods, frequentist methods estimate model parameters, based on some optimal estimate, and use the estimated values in the model. Like Bayesian methods, modern frequentist methods also employ sophisticated sampling techniques for numerical integrations (e.g., de Valpine 2004, Lele et al. 2007) as well as more routine Monte Carlo approaches (e.g., Hornberger and Spear 1981). Commercial software products such as @RISK (Palisade, Ithaca, New York, USA) and Crystal Ball (Oracle, Redwood Shores, California, USA) have made Monte Carlo methods easy to implement in spreadsheet applications. An advantage of using the sampling techniques in modern propagation methods is that the full distribution of the modeled variable is calculated. In contrast, the classical methods can only propagate the first few moments (i.e., s^2, s, or SE, skewness, and elongation) of the normal distribution and the df.

Currently, the state of the art in analyzing uncertainty in ecological problems is hierarchical statistical modeling. Hierarchical models can incorporate the types of uncertainty enumerated above as well as other uncertainties related to sampling design and boundary conditions (Cressie et al. 2009). Thus, hierarchical models have the potential to explicitly account for all of the uncertainty in an ecological analysis. A readable example of hierarchical modeling is presented by Cressie et al. (2009) and in the accompanying Forum discussion in a recent issue of this journal [see Ecological Applications 19(3)]. While hierarchical models are extremely flexible in their ability to encompass all types of uncertainty, the methods for implementing these models are both computationally intensive and technically challenging (Bolker 2009). Both Bayesian (e.g., Cressie et al. 2009) and frequentist (de Valpine 2004, Lele et al. 2007) approaches to hierarchical models have been developed.

As described in this paper, classical uncertainty propagation methods are used to generate confidence intervals for functions of other variables with uncertainty. Lo (2005) further demonstrates how classical methods may be used to propagate both model parameter uncertainty and natural variability in variables. To our knowledge classical methods have not been used in a hierarchical model that includes all of the uncertainties listed by Chatfield (1995), but we do not see any reason why these equations could not be applied in such a context.

Covariance among variables

It is apparent from Eq. 3 that the covariance term, i.e.,

$$2\frac{\partial w}{\partial u}\frac{\partial w}{\partial v}r_{uv}s_u s_v$$

may either increase or decrease the propagated uncertainty. The covariance term will increase the uncertainty if u and v are positively correlated and the product of the partial derivatives is positive. In contrast, the covariance term will decrease the uncertainty in w if u and v are negatively correlated and the product of the partial derivatives is positive or if r_{uv} is positive and one of the partial derivatives is negative.

In our analyses, we have evaluated the covariance between variables based on correlation analysis as well as careful consideration of how we formulated our equations. For example, daily tidal amplitude is calculated as max WSE − min WSE (Appendix F). The populations of max WSE and min WSE are correlated ($r = 0.69$). At the daily time step at which we calculated tidal amplitude, however, max WSE and min WSE are independent of one another and Eq. F.3 does not require the covariance term. Had we instead chosen to calculate the mean daily amplitude (AMP) as $\text{AMP} = \overline{\max \text{WSE}} - \overline{\min \text{WSE}}$ it would have been necessary to include the covariance term. In this example, the partial derivatives $\partial\text{AMP}/\partial\overline{\max \text{WSE}}$ and $\partial\text{AMP}/\partial\overline{\min \text{WSE}}$ would be 1 and −1, respectively. Thus the product of the partial derivatives is negative and covariance term would reduce the uncertainty in mean daily amplitude.

Correlation among variables is also an important consideration in modern approaches to uncertainty. Stow et al. (2007) demonstrate that the parameter space of two correlated variables, x and y, may transcend the limits of the parameter space derived from the ranges in x and y taken individually. Advancements in sampling algorithms such as the Markov chain Monte Carlo have made it much easier to sample from the appropriate parameter space in cases with high correlation among variables. Spatial and temporal correlations within the population of a variable should also be considered (Hoeting 2009).

Methods to estimate variables and derive uncertainty

Table 1 compiles a number of methods to estimate the value and uncertainty of an ecological variable. Starting with direct measurements of a variable (Table 1: method A), examples of location specific measurements (Table 1: method A1) were $[I]$ and $[E]$. These concentrations were measured directly and were used to determine the mean and associated uncertainty. Examples of region specific

measurements (Table 1: method A2) were Pr and [R] at sites representing the region surrounding the studied embayment.

Under method B in Table 1: direct calculations from two or more measured variables (method B1) were exemplified by the viscosity coefficients and the diffusion coefficients for DIN. Under method B2, we include spatial and temporal scaling. In this study, both spatial and temporal scaling relied on external data sources that were specific to our study site. For example, the estimates of embayment area required both the elevation measurements determined from the RTK GPS survey as well as the LIDAR data obtained from Escambia County, Florida. Similarly, the WSEs were a combination of in situ measurements and modeled values based on the NOAA Pensacola tide gauge.

The use of literature variables (Table 1: method C) in the absence of measured variables is ubiquitous in the ecological literature. For example, the calculation of the ratio Dry : Wet for AtmDep (method C1) was based on annual values of Dry : Wet deposition from the literature. However, in the case of BD, which was used to calculate ϕ in the M-Ex term, the best available data set provided only minimum and maximum values for our specific soil type. In this case, a mean and SE were determined using these minimum and maximum values (method C2). This resulted in a large SE, but which approximately encompassed the full error of that mean value.

Method C3 (Table 1) is demonstrated by the determination of the PD of marsh soil through the use of a regression model from the literature (Rühlmann et al. 2006). No values of PD for our site were available, but there were values of the minimum and maximum %OM in the marsh sediment. Hence the Rühlmann et al. (2006) model relating %OM to PD was used to estimate the minimum and maximum PD in our site. When using a regression model from the literature it is important to confirm that the regression model is applicable to the study site. This was so in our case because the data used by the Rühlmann et al. (2006) to develop their regression model encompassed many different types of soils, including ours. Further, Rühlmann et al. (2006) generously provided us with the raw data upon our request. Had our request not been granted, we would have had to digitize the values probably losing some resolution. With the received data from Rühlmann et al. (2006), we could recreate the regression with precision, predict maximum and minimum PD, and calculate the mean PD, SE, and df for our study site.

Another method for estimating an ecological variable is a subjective judgment based on best guesses or first principles (Table 1: method D). Ecological variables are constrained by maximum and minimum values. In the event that there is no direct information about those maximum and minimum values, taking a best guess at possible minimum and maximum values is a way to capture the uncertainty in that variable. For example the molecular weight of DON, which was used to calculate the D_0 for DON, in the marsh sediment of our study site was not known. Using reports from the literature, we chose possible maximum and minimum molecular weight values (see Appendix G). When doing this, we erred towards the liberal side and attempted to capture a range that most likely encompassed the true range of DON molecular weight (Burdige and Gardner 1998, Burdige and Zheng 1998) in the marsh sediment of our study site. In this manner, the uncertainty was not underestimated.

As best we can tell, the method presented here for estimating the uncertainty in the scaling terms A, V, Z, A_{flood}, V_{flood}, and Z_{flood} is novel (Appendix A). Dimensional scalars are frequently used in ecological studies to normalize measurements to similar spatial scales or to extrapolate to ecosystem-wide rates, but potential uncertainties in the estimates of these scalars are also frequently ignored. In many cases dimensional scalars are measured with great accuracy. However, when parameters prone to natural variation, such as WSE, are used to demarcate system boundaries the error in the resulting estimates of dimensional scalars should be propagated and evaluated. The method developed here provides a way to do so.

Uncertainty applications

Flux magnitudes and uncertainties.—An obvious application of uncertainty analyses is the exploratory value for adapting current monitoring designs or for guiding future research strategies. For example, the GW and N-Ex terms were relatively large with large SEs (Fig. 4). Subsequent work should be directed at reducing the uncertainty in these terms. The step-by-step uncertainty propagation procedure employed here offers a template to identify the variables that could contribute most to reducing the uncertainty around GW and N-Ex (Table E1 in Appendix E, Table F1 in Appendix F; see also *Discussion: Uncertainty applications*: *Uncertainty budgets*). PS and M-Ex terms also had large uncertainty relative to their magnitude, but their magnitude was generally negligible in comparison to GW, AtmDep, and N-Ex. Thus, if further monitoring were to occur these terms might be dropped in favor of reducing the uncertainty around GW and monitoring potential sink terms indicated by the large negative Black Box values.

Though, what if no further work is possible? If, for example, the resource manager or scientist is asked to make a recommendation on how to reduce nitrogen loading to this system, the low risk option would be to target AtmDep sources as this term was large in magnitude and was known with more certainty than the other input terms. The larger uncertainties around the N-Ex and GW terms indicate a higher risk that management actions directed at reducing these loading terms would not have the desired effect on the reduction of total nutrient load. A cost-benefit analysis, however, may indicate that the cost of reducing AtmDep from sources

TABLE 2. Uncertainty budgets for the atmospheric deposition (AtmDep), net exchange (N-Ex), and groundwater (GW) flux terms.

Flux term and component	DIN		DON		DIP	
	SE (%)	df (%)	SE (%)	df (%)	SE (%)	df (%)
AtmDep						
P	0.50	0.17	0.31	0.02	0.13	0.001
$[R]$	98.69	99.61	99.21	99.96	24.17	0.32
Dry : Wet	0.81	0.22	0.48	0.020	75.70	99.68
N-Ex						
AMP	0.12	0.00	0.01	0.0	0.31	0.00
$[I]$	70.54	85.25	43.19	39.58	96.03	99.86
$[E]$	29.34	14.75	56.80	60.42	3.65	0.14
GW						
P	0.62	0.17	1.05	8.76	0.74	0.43
ET	47.34	1.01	80.57	51.31	56.83	2.54
[GW]	44.42	98.79	5.41	38.60	33.29	96.96
A_w	7.61	0.03	12.96	1.33	9.14	0.07
A	4×10^{-9}	9×10^{-17}	7×10^{-9}	5×10^{-15}	5×10^{-9}	2×10^{-16}

Notes: Percentage values represent the uncertainty contribution to the total SE and df. Under AtmDep (atmospheric deposition), the contributions of annual precipitation (P), nutrient concentration in the rainfall ($[R]$), and the ratio of dry to wet deposition (Dry : Wet) are shown. Under N-Ex (net exchange [import − export] with the adjacent intercoastal waterway), the contribution of annual cumulative tidal amplitude (AMP) and the import and export nutrient concentrations ($[I]$ and $[E]$) are shown. For the GW (groundwater input) term, the contribution of P, evapotranspiration (ET), groundwater nutrient concentrations ([GW]), recharge area (A_w), and embayment area (A) are shown.

such as power plant and/or vehicle emissions is prohibitive and, thus, N-Ex or GW sources may be targeted. In the end, though, a risk-manager will have some understanding of how effective such measures will be.

Uncertainty budgets.—It is recognized that quantifying the uncertainty in each component of an ecological study or model assists in understanding the results of the study (Reckhow 1994, Borsuk et al. 2004, Lo 2005) and efficiently identifies needs for future descriptive or experimental designs (Lo 2005). Quantitative understanding of error structure may be developed by constructing an error budget (Lo 2005) where Eq. 3, assuming no covariance, is normalized by the total error (SE_w) to give

$$1 = \frac{\left(\frac{\partial w}{\partial u}\right)^2 SE_u^2}{SE_w^2} + \frac{\left(\frac{\partial w}{\partial v}\right)^2 SE_v^2}{SE_w^2}. \quad (23)$$

This normalization quantifies the percent contribution of each variable, in this case u and v where $w = f(u, v)$, to the total error Thus, the variable contributing the most error is easily identified.

We have extended the concept of the error budget to a df budget by rearranging Eq. 7 such that

$$1 = df_w \frac{\left(\frac{\partial w}{\partial u}\right)^4 SE_u^4}{df_u SE_w^4} + df_w \frac{\left(\frac{\partial w}{\partial v}\right)^4 SE_v^4}{df_v SE_w^4}. \quad (24)$$

As opposed to Eq. 23 where the terms on the right side of the equation are contributing additively to SE_w^2, in Eq. 24 the terms are contributing additively to $1/df_w$. While this may, at first glance, seem counterintuitive, if we think of the df as the uncertainty around the SE then it is clear that for large df there is less uncertainty owing to smaller t values. Inversely, small df contribute larger uncertainty. Thus, the $1/df_w$ budget is more heavily weighting the contribution of terms with small df and larger uncertainty.

Exploring the uncertainty budgets of AtmDep, N-Ex, and GW yields some interesting insights (Table 2). For the AtmDep term, $[\bar{R}]$ contributed the most uncertainty in SE and df for DIN and DON, while for DIP Dry : Wet was the greatest contributor to uncertainty. For the N-Ex term, $[\bar{I}]$ accounts for most of the uncertainty in SE and df for DIN, DON, and DIP. The error budget for GW yielded some counterintuitive results regarding which terms most significantly contributed to the total uncertainty. The watershed area (A_w) used in the calculation of GW was 14 434 m^2 with a SE of 3042 m^2 (Appendix E). The SE of this value was large because it was derived as the mean of the minimum and maximum estimated watershed areas. The contribution of A_w to the GW error budget, however, was not the largest (Table 2). ET (1.15 m/yr, SE = 0.15 m/yr, Appendix E) was the largest contributor to the GW SE budget (Table 2) even though the magnitude and SE of ET were seemingly small in comparison to A_w. It is interesting to note that, for the df, there was usually only one term that was dominating the percent contribution to the aggregate term. For example, $[\bar{R}]$ contributed 99.61% to the df of AtmDep. The implication is the df for AtmDep were almost entirely dependent on the df for $[\bar{R}]$. Thus if one wanted to increase the df for AtmDep, an increase in the df for $[\bar{R}]$ would be the best approach.

A further analysis of the uncertainty budget may be undertaken to estimate how reducing errors in input variables translates to error reduction in the resulting term. For example, the SEs of ET and $\left[\overline{GW}\right]$ comprise

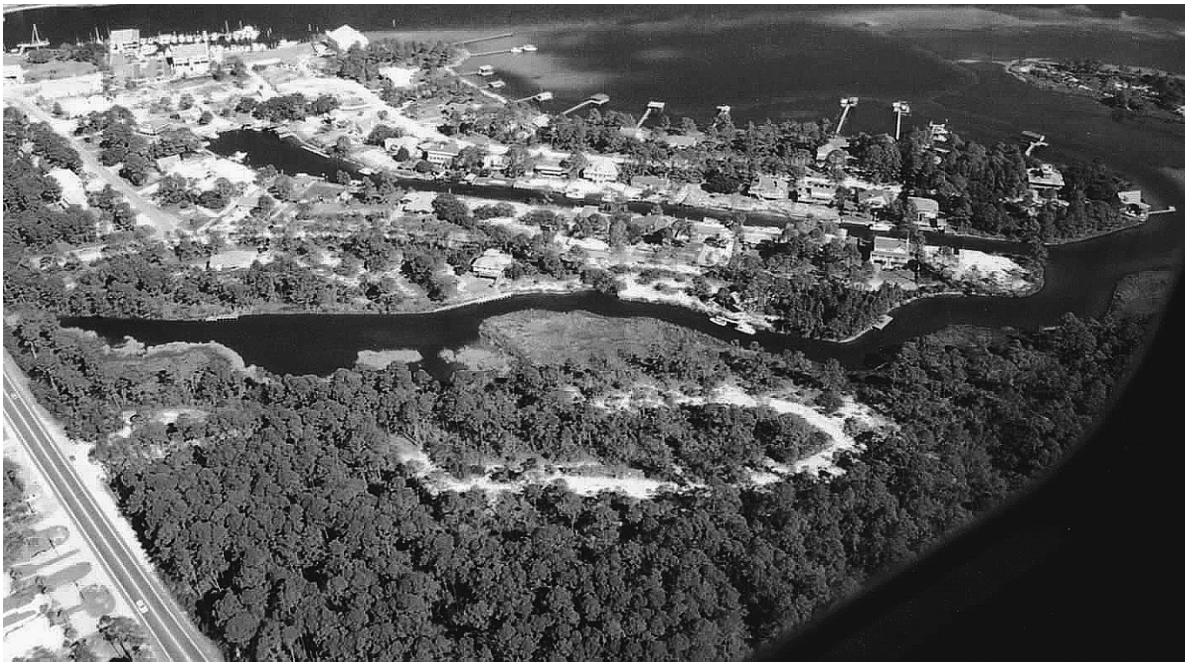

PLATE 1. Aerial photograph of the study site (Gongora lagoon, Florida, USA). Photo credit: Jason Stutes.

58.92 and 9.48% of the error in DIN GW (Table 2). Thus a 1% decrease in SE_{ET} would result in a 0.59% decrease in SE_{GW}. Similarly, a 1% decrease in $SE_{[\overline{GW}]}$ would result in a 0.09% decrease in SE_{GW}. This analysis or sensitivity index (Lo 2005) provides a strategy for how a resource manager or scientist might choose to reduce the uncertainty in a calculated term. In this case, as SE_{ET} is the largest contributor to GW DIN input uncertainty, the best strategy for reducing uncertainty in the GW input would be to improve the accuracy and precision of the ET estimate.

Overall, we have provided a framework for propagating SE and df through a series of step-by-step calculations using both directly measured and subjectively estimated variables. This framework provides for the estimation of uncertainty intervals around calculated values. New contributions to uncertainty propagation methods include uncertainty propagation through GIS computations used for scaling ecological variables, the novel application of uncertainty propagation to ecosystem mass balance budgets, and discussion of management and scientific applications of uncertainty analysis results. The framework for uncertainty propagation presented herein is generally applicable to all ecological studies that use step-by-step and/or scaling calculations. We encourage environmental scientists and managers to use this framework for calculating, assessing, and communicating uncertainty.

ACKNOWLEDGMENTS

We thank Jason Stutes, Amy Hunter, Alina Corcoran, Adrienne Stutes, and the technical support staff of the Dauphin Island Sea Lab for their field and analytical work. Critical reviews provided by Ernest Lo and an anonymous reviewer greatly improved this manuscript. We gratefully acknowledge the data provided by Jorge Rühlmann, which were used to calculate marsh sediment particle density. Some data used in this publication were provided by the Virginia Coast Reserve LTER project, which was supported by National Science Foundation grants BSR-8702333-06, DEB-9211772, DEB-9411974, and DEB-0080381. This research was partially funded by grants to J. Cebrian from Alabama Center for Estuarine Studies (ACES, grant #5-21854) and the National Coastal Data Development Center (NOAA, grant #NA06OAR4320264) and by support for J. Lehrter by the U.S. EPA, National Health and Environmental Effects Laboratory. The contents are solely the views of the authors. Use of trade names or commercial products does not constitute endorsement by the U.S. EPA. This is contribution 1345 from the U.S. EPA Gulf Ecology Division.

LITERATURE CITED

Ahn, H., and R. T. James. 2001. Variability, uncertainty, and sensitivity of phosphorus deposition load estimates in South Florida. Water, Air, and Soil Pollution 126:37–51.

Alperin, M. J., W. S. Reeburgh, and A. H. Devol. 1992. Organic carbon remineralization and preservation in sediments of Skan Bay, Alaska. Pages 99–122 *in* J. K. Whelan and J. Farrington, editors. Organic matter: productvity, accumulation, and preservation in recent and ancient sediments. Columbia University Press, New York, New York, USA.

Anderson, K. A., and J. A. Downing. 2006. Dry and wet atmospheric deposition of nitrogen, phosphorus, and silicon in an agricultural region. Water, Air, and Soil Pollution 176: 351–374.

Berner, R. A. 1980. Early diagenesis: a theoretical approach. Princeton University Press, Princeton, New Jersey, USA.

Birge, R. T. 1939. The propagation of errors. American Physics Teacher 6:351–357.

Bolker, B. 2009. Learning hierarchical models: advice for the rest of us. Ecological Applications 19:588–592.

Borsuk, M. A., C. A. Stow, and K. H. Reckhow. 2004. A Bayesian network of eutrophication models for synthesis, prediction, and uncertainty analysis. Ecological Modelling 173:219–239.

Boudreau, B. P. 1996. The diffusive tortuosity of fine-grained unlithified sediments. Geochimica et Cosmochimica Acta 60: 3139–3142.

Boudreau, B. P. 1997. Diagenetic models and their implementation. Springer-Verlag, Berlin, Germany.

Boynton, W. R., J. D. Hagy, J. C. Cornwell, W. M. Kemp, S. M. Greene, M. S. Owens, J. E. Baker, and R. K. Larsen. 2008. Nutrient budgets and management actions in the Patuxent River Estuary, Maryland. Estuaries and Coasts 31: 623–651.

Brewer, C. A., and L. J. Gross. 2003. Training ecologists to think with uncertainty in mind. Ecology 84:1412–1414.

Burdige, D. J., and K. G. Gardner. 1998. Molecular weight distribution of dissolved organic carbon in marine sediment porewaters. Marine Chemistry 62:45–64.

Burdige, D. J., and S. Zheng. 1998. The biogeochemical cycling of dissolved organic nitrogen in estuarine sediments. Limnology and Oceanography 43:1796–1813.

Chatfield, C. 1995. Model uncertainty, data mining, and statistical inference. Journal of the Royal Statistical Society A 158:419–466.

Cressie, N., C. A. Calder, J. S. Clark, J. M. Ver Hoef, and C. K. Wikle. 2009. Accounting for uncertainty in ecological analysis: the strengths and limitations of hierarchical statistical modeling. Ecological Applications 19:553–570.

D'Elia, C. F., P. A. Steudler, and N. Corwin. 1977. Determination of total nitrogen in aqueous samples using persulfate digestion. Limnology and Oceanography 22:760–764.

de Valpine, P. 2004. Monte Carlo state-space likelihoods by weighted posterior kernel density estimation. Journal of the American Statistical Association 99:523–536.

de Valpine, P. 2009. Shared challenges and common ground for Bayesian and classical analysis of hierarchical statistical models. Ecological Applications 19:554–588.

Dingman, S. L. 1994. Physical hydrology. Prentice Hall, Upper Saddle River, New Jersey, USA.

Gilks, W. R., A. Thomas, and D. J. Spiegelhalter. 1994. A language and programming for complex Bayesian modeling. Statistician 43:169–177.

Hall, B. D., and R. Willink. 2001. Does "Welch-Satterthwaite" make a good uncertainty estimate? Metrologia 38:9–15.

Halpern, B. S., H. M. Regan, H. P. Possingham, and M. A. McCarthy. 2006. Accounting for uncertainty in marine reserve design. Ecology Letters 9:2–11.

Hoeting, J. A. 2009. The importance of accounting for spatial and temporal correlation in analyses of ecological data. Ecological Applications 19:574–577.

Hornberger, G. M., and R. C. Spear. 1981. An approach to the preliminary analysis of environmental systems. Journal of Environmental Management 12:7–18.

International Organization for Standardization. 1995. Guide to the expression of uncertainty in measurement (GUM). ISO/IEC Guide 98:1995. International Organization for Standardization, Geneva, Switzerland.

Jost, W. 1960. Diffusion in solids, liquids, and gases. Academic Press, New York, New York, USA.

Kostka, J. E., B. Gribsholt, E. Peterie, D. Dalton, H. Skelton, and E. Kristensen. 2002. The rates and pathways of carbon oxidation in bioturbated saltmarsh sediments. Limnology and Oceanography 47(1):230–240.

Ku, H. 1966. Notes on the use of propagation of error formulas. Journal of Research of the National Bureau of Standards C. Engineering and Instrumentation 70(C): 263–273.

Lele, S. R., B. Dennis, and F. Lutscher. 2007. Data cloning: easy maximum likelihood estimation for complex ecological models using Bayesian Markov chain Monte Carlo methods. Ecology Letters 10:551–563.

Li, Y., and S. Gregory. 1974. Diffusion of ions in sea water and in deep-sea sediments. Geochimica et Cosmochimica Acta 38: 703–714.

Lo, E. 2005. Gaussian error propagation applied to ecological data: post-ice-storm-downed wood biomass. Ecological Monographs 75:451–466.

Lu, J., G. Sun, S. G. McNulty, and D. M. Amatya. 2005. A comparison of six potential evapotransopiration methods for regional use in the Southeastern United States. Journal of the American Water Resources Association 41(3): 621–633.

McKee, K. L., I. A. Mendelssohn, and M. D. Materne. 2006. Salt marsh dieback in coastal Louisiana: Survey of plant and soil conditions in Barataria and Terrebonne Basins, June 2000–September 2001. USGS Open-File Report 2006-1167. U.S. Geological Survey, Reston, Virginia, USA.

Meyers, T., J. Sickles, R. Dennis, K. Russell, J. Galloway, and T. Church. 2001. Atmospheric nitrogen deposition to coastal estuaries and their watersheds. Pages 53–76 *in* R. A. Valigura, R. B. Alexander, M. S. Castro, T. P. Meyers, H. W. Paerl, P. E. Stacey, and R. E. Turner, editors. Nitrogen loading in coastal water bodies: an atmpospheric perspective. American Geophysical Union, Washington, D.C., USA.

Millero, F. J., and A. Poisson. 1981. Summary of data treatment for the Unesco one atmosphere equation of state for seawater. Deep-Sea Research 28A:625–629.

Peters, N. E., and R. S. Reese. 1995. Variations of weekly atmospheric deposition for multiple collectors at a site on the shore of Lake Okeechobee, Florida. Atmospheric Environment 29:179–187.

Reckhow, K. H. 1994. Water quality simulation modeling and uncertainty analysis for risk assessment and decision making. Ecological Modelling 7:1–20.

Regan, H. M., M. Colyvan, and M. A. Burgman. 2002. A taxonomy and treatment of uncertainty for ecology and conservation biology. Ecological Applications 12:618–628.

Rühlmann, J., M. Körschens, and J. Graefe. 2006. A new approach to calculate the particle density of soils considering properties of the soil organic matter and the mineral matrix. Geoderma 130:272–283.

Satterthwaite, F. E. 1941. Synthesis of variance. Psychometrika 6:309–316.

Sharp, J. H. 1974. Improved analysis for "particulate" organic carbon and nitrogen from seawater. Limnology and Oceanography 19:984–989.

Sokal, R. M., and F. J. Rohlf. 1995. Biometry. Third edition. W. H. Freeman and Company, New York, New York, USA.

Stow, C. A., K. H. Reckhow, S. S. Qian, E. C. Lamon III, G. B. Arhonditsis, M. E. Borsuk, and D. Seo. 2007. Approaches to evaluate water quality model parameter uncertainty for adaptive TMDL implementation. Journal of the American Water Resources Association 43:1499–1507.

Strickland, J. D., and T. R. Parsons. 1972. A practical handbook of seawater analysis. Fisheries Research Board of Canada, Ottawa, Ontario, Canada.

Stutes, J., J. Cebrian, A. L. Stutes, A. Hunter, and A. A. Corcoran. 2007. Benthic metabolism across a gradient of anthropogenic impact in three shallow coastal lagoons in NW Florida. Marine Ecology Progress Series 348:55–70.

Taylor, B. N., and C. E. Kuyatt. 1994. Guidelines for evaluating and expressing the uncertainty of NIST measure-

ment results. Technical note 1297. National Institute of Standards and Technology, Washington, D.C., USA.

Tukey, J. W. 1956. The propagation of errors, fluctuations, and tolerances. Unpublished technical reports. Princeton University, Princeton, New Jersey, USA.

Tyler, A. C., and J. C. Zieman. 1997. VCR97014: Creekbank physico-chemical data from Hog Island salt marsh chronosequence. Virginia Coast Reserve Long-Term Ecological Research Project, Charlottesville, Virginia, USA.

UNESCO. 1983. Algorithms for computation of fundamental properties of seawater. UNESCO technical papers in marine science 44. UNESCO, Paris, France.

Welch, B. L. 1947. The generalization of "Student's" problem when several different population variances are involved. Biometrika 34:28–35.

APPENDIX A

Uncertainty assessment for annual mean embayment area, volume, and depth (*Ecological Archives* A020-015-A1).

APPENDIX B

Uncertainty assessment for change in storage (ΔS) (*Ecological Archives* A020-015-A2).

APPENDIX C

Uncertainty assessment for atmospheric deposition (AtmDep) (*Ecological Archives* A020-015-A3).

APPENDIX D

Uncertainty assessment for point source input (PS) (*Ecological Archives* A020-015-A4).

APPENDIX E

Uncertainty assessment for groundwater input (GW) (*Ecological Archives* A020-015-A5).

APPENDIX F

Uncertainty assessment for net exchange (N-Ex) (*Ecological Archives* A020-015-A6).

APPENDIX G

Uncertainty assessment for marsh exchange (M-Ex) (*Ecological Archives* A020-015-A7).

APPENDIX H

Uncertainty assessment for the Black Box (BB) terms (*Ecological Archives* A020-015-A8).